High-resolution study of excited 0^{+} states in ^{200}Hg and ^{202}Hg

C. Bernards, R. F. Casten, V. Werner, P. von Brentano, D. Bucurescu, G. Graw, S. Heinze, R. Hertenberger, J. Jolie, S. Lalkovski, D. A. Meyer, D. Mücher, P. Pejovic, C. Scholl, and H.-F. Wirth

High-resolution study of excited 0^+ states in ^{200}Hg and ^{202}Hg

C. Bernards*,[1] R.F. Casten,[1] V. Werner,[1] P. von Brentano,[2] D. Bucurescu,[3] G. Graw,[4] S. Heinze,[2]
R. Hertenberger,[4] J. Jolie,[2] S. Lalkovski,[5] D.A. Meyer,[1] D. Mücher†,[2] P. Pejovic,[2] C. Scholl,[2] and H.-F. Wirth[6]

[1]*Wright Nuclear Structure Laboratory, Yale University, New Haven, CT-06520, USA*
[2]*Institut für Kernphysik, Universität zu Köln, D-50937 Köln, Germany*
[3]*National Institute for Physics and Nuclear Engineering, Bucharest, R-76900, Romania*
[4]*Fakultät für Physik, Ludwig-Maximilians-Universität München, D-85748 Garching, Germany*
[5]*Faculty of Physics, University of Sophia, 1164 Sofia, Bulgaria*
[6]*Physik Department, Technische Universität München, D-85748 Garching, Germany*
(Dated: June 18, 2013)

We used the high-resolution Q3D magnetic spectrograph at the Maier-Leibnitz Laboratory (MLL) Tandem accelerator in Munich to study ^{200}Hg and ^{202}Hg after two-neutron transfer. The results confirm the sharp drop in the number of low-lying 0^+ states towards the ^{208}Pb shell closure. In total, we assigned six 0^+ states in ^{200}Hg and four 0^+ states in ^{202}Hg. The 0^+ excitation energies and the measured (p, t) transfer cross sections indicate a structural change throughout the Hg isotopes, with the most notable result being the peaking in the cross section of the 0_2^+ state in ^{200}Hg.

PACS numbers: 21.10.Re, 21.60.Ev, 25.40.Hs, 27.80.+w

I. INTRODUCTION

Within the last decade, much work has been done to investigate 0^+ excitations in nuclei using the high-resolution Q3D magnetic spectrograph [1] at the Maier-Leibnitz Laboratory (MLL) Tandem accelerator in Munich. The Q3D spectrograph with its focal plane detector [2] has turned out to be a very powerful tool for the identification of 0^+ states by measuring the characteristic forward peaking of $L = 0$ transfers (Ref. [3] gives an overview of two-nucleon stripping or pickup transfer reactions).

The (p, t) pickup transfer reaction has been studied in an extensive campaign in the rare earth region [4–9] from Gd to Hg. This research has allowed a better understanding of the changes the nuclei undergo from the transitional Gd region – over the well-deformed Yb region – to the γ-soft Pt region and further towards the ^{208}Pb proton-neutron shell closure. The striking high number of low-lying 0^+ excitations in the Gd region [4, 5] was interpreted [10] as a new signature for shape-phase transitions [11] and large numbers of 0^+ states throughout the rare earth region triggered many calculations reproducing the surprisingly high 0^+ density [12–15]. The latest experiments on ^{192}Pt, ^{194}Pt [8], and ^{198}Hg [9] showed a rather smooth decline in 0^+ state density towards the proton-neutron shell closure. This decline was found to be in qualitative agreement with sd IBM-1 calculations [9], and in line with expectations based on the reduced shell model valence spaces as the magic region is approached.

By investigating excited 0^+ states in ^{200}Hg and ^{202}Hg, we move further towards the shell closure. The new high-resolution data allows us to compare excited 0^+ states throughout the mercury isotope chain from ^{198}Hg to ^{202}Hg and enables us to inspect their evolution. The present paper completes the publication of all the existing data from the (p, t) campaign from Gd to Hg that was carried out using the ultra-high resolution instrument in Munich.

II. EXPERIMENT

The (p, t) transfer experiments investigating ^{200}Hg and ^{202}Hg were performed at the Munich MLL (Maier-Leibnitz Laboratory of LMU Munich and TU Munich) Tandem accelerator facility. We used highly enriched mercury-sulfide targets consisting of 50-μg/cm^2 ^{202}HgS on a 10-μg/cm^2 carbon backing, and 70-μg/cm^2 ^{204}HgS on a 12-μg/cm^2 carbon backing, respectively. The isotopic composition of the ^{202}Hg target was ^{202}Hg (97.58%), ^{201}Hg (1.38%), ^{200}Hg (0.53%), ^{204}Hg (0.28%), ^{199}Hg (0.17%), ^{198}Hg (0.06%), and ^{196}Hg ($< 0.02\%$), whereas the ^{204}Hg target consisted of ^{204}Hg (92.64%), ^{202}Hg (4.85%), ^{200}Hg (0.90%), ^{201}Hg (0.76%), ^{199}Hg (0.56%), ^{198}Hg (0.28%), and ^{196}Hg ($< 0.05\%$).

These experiments on ^{200}Hg and ^{202}Hg were part of the same Q3D (p, t) transfer campaign as the ^{198}Hg measurement [9] using an ultra-high resolution setup consisting of the Q3D magnetic spectrograph [1] and the high-resolution

---

focal-plane detector described in Ref. [2], with typical triton energy resolution at 3-5 keV. The beam energy of the unpolarized protons was 25 MeV and the outgoing triton distribution was measured at 5°, 17.5°, and 30° laboratory angle with respect to the beam axis. Each angle was measured with two different magnetic settings in order to resolve the tritons with an acceptable energy resolution up to 3-MeV excitation energy. For the analysis, the six different runs (three angles, each with two magnetic settings) were normalized to the integrated beam current measured in a Faraday cup behind the target.

III. ANALYSIS

Since the characteristic (p,t) angular distribution strongly peaks in the forward direction solely for $L = 0$ transfers [5], we use the ratio $R(5/17.5) \equiv \sigma(5°)/\sigma(17.5°)$ to identify $L = 0$ transfers from the 0^+ ground state in ^{202}Hg to 0^+ states in ^{200}Hg, or the 0^+ ground state ^{204}Hg to 0^+ states in ^{202}Hg. We use a ratio $R(5/17.5) > 3$ as a safe lower limit for 0^+ states assignments [7, 9]. The 30° data is used for the peak identification, but is not necessary for a clean separation of 0^+ states from 2^+ or 4^+ states [5].

For each nucleus, the experimental runs were normalized to the integrated beam current measured in a Faraday cup behind the target. The measured triton spectra were calibrated using well-known level energies of ^{200}Hg and ^{202}Hg compiled in the Nuclear Data Sheets [16, 17]. Contaminants stemming from target impurities were identified by using the known Q values of the corresponding (p,t) transfer reaction [18]. In total, about 80 individual excited states were analyzed up to the $\sim$ 3-MeV excitation-energy for ^{200}Hg and ^{202}Hg.

IV. RESULTS FOR ^{200}HG

Figure 1 shows the 5° laboratory angle spectrum measured with two different magnetic settings covering the low-energy (LE) and high-energy (HE) part of the spectrum. All runs were normalized to the 5° LE run. Some intense peaks are cut off and labeled with a multiplying factor representing their real maximum height.

Based on the $R(5/17.5) = 3$ limit, six states are assigned as 0^+ states in ^{200}Hg and listed in Table I. The respective $R(5/17.5)$ ratios are plotted in Fig. 2. A complete list of all states analyzed in the ^{200}Hg runs and their cross sections at 5°, 17.5°, and 30° laboratory angles is given in Table II.

The first four 0^+ states in Table I up to 1857-keV excitation energy were already known as 0^+ states [16] and we confirm their spin assignment. We observe two more states clearly exceeding the $R(5/17.5) = 3$ limit: One state at 2246-keV excitation energy is observed with $R(5/17.5) = 4.97(68)$. In the Nuclear Data Sheets [16], the spin of this state is given as $J^\pi = (1,2)^+$, based on the measured mixed $M1 + E2$ multipolarity of its γ-ray transition to a 1^+ state [19]. The observed mixed multipolarity in Ref. [19] conflicts with our 0^+ state assignment. We checked potential 0^+ states using $\gamma\gamma$ coincidence data on ^{200}Hg which was taken in a recent cold neutron capture experiment at Institut Laue-Langevin (ILL) [20] – and which has also been used in a recent paper [21] –. Due to statistics, we were not able to determine the multipole mixing ratio of the transition connecting the 2246-keV and the 1570-keV 1^+ state using the ILL data and did not find a reason for this particular discrepancy. Another new 0^+ state is observed at 2475 keV.

At 2332-keV excitation energy, a state exceeds the $R(5/17.5) = 3$ limit with relatively large uncertainties. In the data sheets [16], the level spin is listed as $J = 2^+$ and an observed γ-ray transition to a 4^+ state rules out a possible spin $J = 0^+$ assignment. However, according to the $\gamma\gamma$ coincidence data from ILL [20, 21], the 1385.0-keV transition to the 4^+ state is incorrectly placed in the level scheme. Gating on the feeding primary γ-ray transition of the 2332-keV level does not show a depopulating 1385-keV γ-ray. A gate on the feeding primary γ-ray to the level at 2978-keV excitation energy, however, does reveal a new 1385-keV transition to the 1593-keV 2^+ state. This state decays by a 646-keV transition to the 947-keV 4_1^+ state, thus making the 1385-keV γ-ray transition coincident with the $4_1^+ \to 2_1^+$ transition. This might have caused the incorrect placement of the 1385-keV γ-ray in the level scheme between the level at 2332 keV and the 4_1^+ state at 947-keV excitation energy [16], although this placement is questioned in Fig. 6 of Ref. [19] as well. Given the large uncertainties of the $R(5/17.5)$ ratio, we tentatively assign spin (0^+) for the state at 2332 keV.

We cannot confirm the 0^+ assignment for the state at 2116.5 keV [16]. Although the assignment is based on the observed $E0$ transition to the 0^+ ground state [22], our measured ratio $R(5/17.5) = 0.58(16)$ does not allow a 0^+ assignment since this state does not show the typical forward-peaking expected for a $L = 0$ transfer.

V. RESULTS FOR ^{202}HG

We were able to assign four 0^+ states based on the $R(5/17.5)$ ratio in ^{202}Hg. They are marked in the 5° spectra shown in Fig. 3 and listed in Table III. Similar to the ^{200}Hg measurement, data were taken in six different runs and normalized to the ^{202}Hg 5° low-energy (LE) run. A detailed list of all states investigated and their respective cross sections is given in Table IV.

Three of these 0^+ states were known as 0^+ states previously [17]. The state at 2599 keV has not been reported before and shows the typical $L = 0$ transfer signature with $R(5/17.5) = 4.25(39)$. There are five more states shown in Fig. 4 at or above the $R(5/17.5) = 3$ limit, but within that limit given their 1σ error-bars, at 1656, 1779, 2127, 2571, and 2685-keV excitation energy. They all have small cross sections (≤ 0.006 mb/sr at 17.5°) and their uncertainties prevent us from firm spin assignments. Out of the five states, only the state at 2127-keV excitation energy was observed before and was assigned spin $J = (2^+)$ [17]. For firm assignments, more statistics is needed so we can only assign tentative spin $J = (0^+)$ for these states, being well aware that these tentative assignments might simply be caused by the low statistics for these states. Our data do not confirm a tentative (0^+) assignment of a state at 1565 keV in Ref. [23] and a 0^+ assignment for a state at 1901-keV excitation energy in Ref. [24]. In both cases, we do not observe the typical forward-peaking signature for the expected $L = 0$ transfer and measured $R(5/17.5) = 1.10(8)$ for the 1565-keV and $R(5/17.5) = 1.54(28)$ for the 1901-keV state.

VI. DISCUSSION

The new high-resolution data on 0^+ excitations in ^{200}Hg and ^{202}Hg completes the data from the present Q3D (p,t) transfer experiments and allows us to move closer to the proton-neutron shell closures at ^{208}Pb. In Ref. [9], we inspected the density of low-energy 0^+ states as a function of valence nucleons $N_{\rm val}$ and concluded that the low number of 0^+ states in ^{198}Hg seem to be due to the approach to the ^{208}Pb shell closure. Here we find, consistently, that the numbers of firm 0^+ assignments in ^{200}Hg and ^{202}Hg are comparably low. The new data is added to Fig. 5 (cf. Fig. 5 in Ref. [9]). One notes that the new data on ^{200}Hg and ^{202}Hg, $N_{\rm val} = 8$ and 6, respectively, is still well described by the total number of sd IBM states [25]. The number of experimentally observed 0^+ states below 3 MeV in the Hg isotopes ranging from $N_{\rm val} = 6$ to 10 shows a rather unsteady behavior though and may show a small peak at ^{200}Hg.

In Fig. 6 we plot the energies of the firmly assigned 0^+ excitations for $^{198-202}$Hg. Besides the larger number of observed 0^+ states in ^{200}Hg one notes a considerable rise in the excitation energy of the assigned 0_4^+ state in ^{202}Hg at $N_{\rm val} = 6$. The effect vanishes if one considers the tentatively assigned (0^+) state at 1779 keV ($\sim 1\sigma$ above $R(5/17.5) = 3$ limit in Fig. 2) as 0_4^+. In that case, the 0_3^+ and 0_4^+ energies are about constant throughout the Hg nuclei studied, only the 0_2^+ energy showing a distinct drop in ^{200}Hg at $N_{\rm val} = 8$. In addition to the 0_2^+ level energies, one also notes an anomalous behavior of the 2_2^+ and 4_1^+ state energies in comparison with neighboring Hg isotopes shown in Fig. 7.

The distinctive nature of the 0_2^+ state in ^{200}Hg becomes more apparent when comparing the relative observed cross sections of the 0^+ states observed in the Hg isotopes. Figure 8 shows the relative observed cross section $\Sigma_i \sigma_n(i)/\Sigma_i \sigma_1(i)$, with $i = 5°, 17.5°$, or 30° and $n > 1$, for the assigned 0_n^+ states in ^{198}Hg, ^{200}Hg, and ^{202}Hg as a function of the number of valence nucleons $N_{\rm val}$. One immediately notes the large relative cross section for the 0_2^+ state in ^{200}Hg at $N_{\rm val} = 8$. The cross section of this state is far stronger than of any other excited 0^+ state observed in these isotopes. Historically, 0^+ state two-nucleon transfer cross sections approaching or exceeding 15% of the ground-state cross section have signaled special structural effects such as phase transitional regions (Sm, Gd), shape coexistence, or special pairs modes (actinides) [11, 27–31]. For the Hg isotopes investigated, the strongest relative

cross section to an excited 0^+ state in the forward direction is 3% for ^{198}Hg [9], peaking at 12% for ^{200}Hg, and 7% ^{202}Hg (cf. Fig. 8 in Ref. [11]). The relative observed 0_3^+ cross section smoothly declines with $N_{\rm val}$, whereas the 0_4^+ cross section remains constant for the Hg isotopes investigated.

The origin of the enhanced $\sigma(0_2^+)$ value in ^{200}Hg is not clear. It has been associated with an oblate single particle energy gap [24] but other explanations such as mixing or coexistence cannot be ruled out. We note that the two-neutron separation energy S_{2n} shows at most a weak anomaly (visible in the differential δS_{2n}) [32, 33].

VII.   CONCLUSION

The (p, t) transfer experiments on ^{200}Hg and ^{202}Hg complete the current Q3D (p, t) campaign of 15 nuclei in the rare-earth region with new results in a near-magic region where we confirm the sharp drop of low-lying 0^+ states compared to transitional and deformed regions.

By comparing the even Hg isotopes, we note the strong anomalous behavior of the low-energy states – especially the 0_2^+ state – in ^{200}Hg. The 0_2^+ excitation energy is significantly lower than for the neighboring 0_2^+ states, whereas its relative cross section (to the ground state) is higher than the relative cross sections measured for the 0_2^+ states in ^{198}Hg and ^{202}Hg. The properties of the low-energy states in ^{200}Hg should definitely be further investigated, e.g., by measuring transition strengths between the low-lying states, to learn more about their special character.

VIII.   ACKNOWLEDGMENTS

[1] M. Löffler, H.J. Scheerer, and H. Vonach, Nucl. Instr. Methods **111**, 1 (1973).
[2] H.-F. Wirth, Ph.D. thesis, Technische Universität München, 2001 [http://tumb1.biblio.tu-muenchen.de/publ/diss/ph/2001/wirth.html].
[3] R.A. Broglia, O. Hansen, and C. Riedel, Adv. Nucl. Phys. 6, 287 (1973).
[4] S.R. Lesher, A. Aprahamian, L. Trache, A. Oros-Peusquens, S. Deyliz, A. Gollwitzer, R. Hertenberger, B.D. Valnion, and G. Graw Phys. Rev. C **66**, 051305(R) (2002).
[5] D.A. Meyer, V. Wood, R.F. Casten, C.R. Fitzpatrick, G. Graw, D. Bucurescu, J. Jolie, P. von Brentano, R. Hertenberger, H.-F. Wirth, N. Braun, T. Faestermann, S. Heinze, J.L. Jerke, R. Krücken, M. Mahgoub, O. Möller, D. Mücher, and C. Scholl Phys. Rev. C **74**, 044309 (2006).
[6] D. Bucurescu, G. Graw, R. Hertenberger, H.-F. Wirth, N. Lo Iudice, A.V. Sushkov, N.Yu. Shirikova, Y. Sun, T. Faestermann, R. Krücken, M. Mahgoub, J. Jolie, P. von Brentano, N. Braun, S. Heinze, O. Möller, D. Mücher, C. Scholl, R.F. Casten, and D.A. Meyer, Phys. Rev. C **73**, 064309 (2006).
[7] L. Bettermann, S. Heinze, J. Jolie, D. Mücher, O. Möller, C. Scholl, R.F. Casten, D.A. Meyer, G. Graw, R. Hertenberger, H.-F. Wirth, and D. Bucurescu, Phys. Rev. C **80**, 044333 (2009).
[8] G. Ilie, R.F. Casten, P. von Brentano, D. Bucurescu, T. Faestermann, G. Graw, S. Heinze, R. Hertenberger, J. Jolie, R. Krücken, D.A. Meyer, D. Mücher, C. Scholl, V. Werner, R. Winkler, and H.-F. Wirth, Phys. Rev. C **82**, 024303 (2010).
[9] C. Bernards, R.F. Casten, V. Werner, P. von Brentano, D. Bucurescu, G. Graw, S. Heinze, R. Hertenberger, J. Jolie, S. Lalkovski, D.A. Meyer, D. Mücher, P. Pejovic, C. Scholl, and H.-F. Wirth, Phys. Rev. C **87**, 024318 (2013).
[10] D.A. Meyer, V. Wood, R.F. Casten, C.R. Fitzpatrick, G. Graw, D. Bucurescu, J. Jolie, P. von Brentano, R. Hertenberger, H.-F. Wirth, N. Braun, T. Faestermann, S. Heinze, J.L. Jerke, R. Krücken, M. Mahgoub, O. Möller, D. Mücher, and C. Scholl, Phys. Lett. **B638**, 44 (2006).
[11] P. Cejnar, J. Jolie, and R.F. Casten, Rev. Mod. Phys. **82**, 2155 (2010).
[12] N.V. Zamfir, Jing-ye Zhang, and R.F. Casten, Phys. Rev. C **66**, 057303 (2002).
[13] Yang Sun, Ani Aprahamian, Jing-ye Zhang, and Ching-Tsai Lee, Phys. Rev. C **68**, 061301(R) (2003).
[14] N. Lo Iudice, A.V. Sushkov, and N.Yu. Shirikova, Phys. Rev. C **70**, 064316 (2004).
[15] N. Lo Iudice, A.V. Sushkov, and N.Yu. Shirikova, Phys. Rev. C **72**, 034303 (2005).

[16] F.G. Kondev and S. Lalkovski, Nuclear Data Sheets **108**, 1471 (2007).
[17] S. Zhu and F.G. Kondev, Nuclear Data Sheets **109**, 699 (2008).
[18] Q-value Calculator (QCalc) [`http://www.nndc.bnl.gov/qcalc/`].
[19] D. Breitig, R.F. Casten, and G.W. Cole, Phys. Rev. C **9**, 366 (1974).
[20] W. Urban, M. Jentschel, B. Märkisch, T. Materna, Ch. Bernards, C. Drescher, C. Fransen, J. Jolie, U. Köster, P. Mutti, T. Rzaca-Urban, and G.S. Simpson, JINST **8**, P03014 (2013).
[21] C. Bernards, W. Urban, M. Jentschel, B. Märkisch, J. Jolie, C. Fransen, U. Köster, T. Materna, G.S. Simpson, and T. Thomas, Phys. Rev. C **84**, 047304 (2011).
[22] A.R.H. Subber, W.D. Hamilton, and G. Colvin, J. Phys. G: Nucl. Phys. **13**, 1299 (1987).
[23] D. Breitig, R.F. Casten, W.R. Kane, G.W. Cole, and J.A. Cizewski, Phys. Rev. C **11**, 546 (1975).
[24] M. Vergnes, G. Berrier-Ronsins, G. Rotbard, J. Skalski, and W. Nazarewicz, Nucl. Phys. **A514**, 381 (1990).
[25] F. Iachello and A. Arima, *The Interacting Boson Model* (Cambridge University Press, Cambridge, UK, 1987).
[26] C. Bernards, Ph.D. thesis, Universität zu Köln, *Investigation and supersymmetric description of even-even mercury isotopes* (Verlag Dr. Hut, Munich, GER, 2011).
[27] S. Hinds, J.H. Bjerregaard, O. Hansen, and O. Nathan, Phys. Lett. **B14**, 48 (1965).
[28] J.H. Bjerregaard, O. Hansen, O. Nathan, and S. Hinds, Nucl. Phys. **86**, 145 (1966).
[29] D.G. Fleming, C. Günter, G.B. Hagemann, B. Herskind, and P.O. Tjøm, Phys. Rev. Lett. **27**, 1235 (1971).
[30] M.A. Oothoudt, and N.M. Hintz, Nucl. Phys. **A213**, 221 (1973).
[31] J.V. Maher, J.R. Erskine, A.M. Friedman, R.H. Siemssen, and J.P. Schiffer, Phys. Rev. C **5**, 1380 (1972).
[32] S. Anghel, G. Cata-Danil, and N.V. Zamfir, Rom. J. Phys. **54**, 301 (2009).
[33] R.B. Cakirli, R.F. Casten, and K. Blaum, Phys. Rev. C **82**, 061306(R) (2010).

Figures
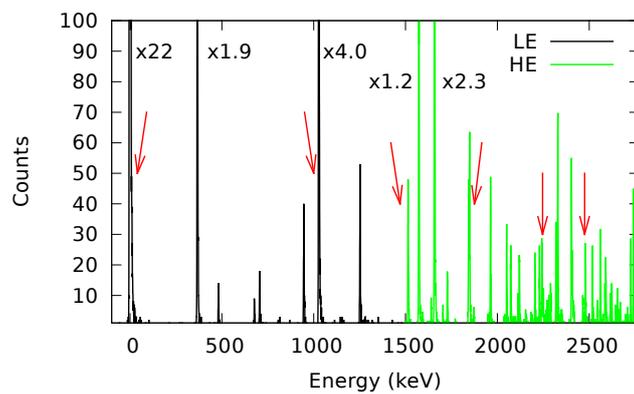
FIG. 1: (Color online) Complete triton spectrum from 0 to ∼ 3-MeV excitation energy, measured at 5° laboratory angle. The intensity of the high-energy (HE) part of the spectrum is normalized to the low-energy (LE) part. The arrows mark the 0^+ state assignments in ^{200}Hg based on the $R(5/17.5)$ ratio.
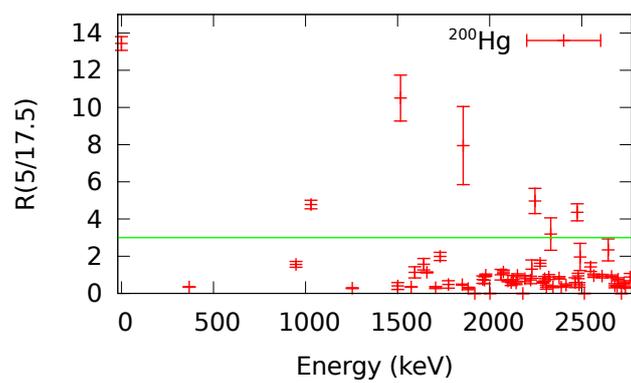
FIG. 2: (Color online) Ratio $R(5/17.5)$ used to assign 0^+ states in ^{200}Hg. The green line marks the $R(5/17.5) = 3$ threshold that is used as a lower limit for 0^+ assignments.
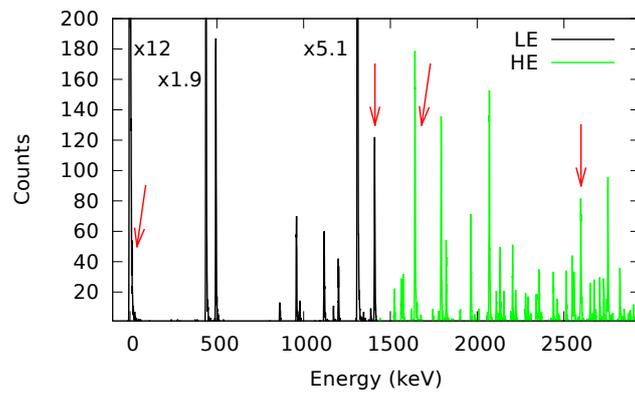
FIG. 3: (Color online) Complete triton spectrum from 0 to $\sim$ 3-MeV excitation energy, measured at $5°$ laboratory angle. The intensity of the high-energy (HE) part of the spectrum is normalized to the low-energy (LE) part. The arrows mark the 0^+ state assignments in ^{202}Hg based on the $R(5/17.5)$ ratio.
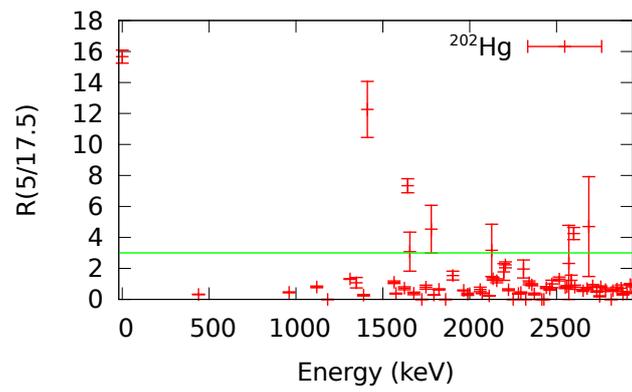
FIG. 4: (Color online) Ratio $R(5/17.5)$ used to assign 0^+ states in ^{202}Hg. The green line marks the $R(5/17.5) = 3$ threshold that is used as a lower limit for 0^+ assignments.
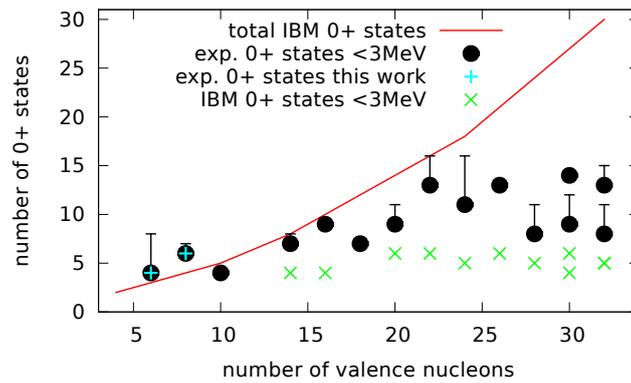
FIG. 5: (Color online) Number of 0^+ states up to 3-MeV excitation energy for the nuclei investigated in this Q3D (p,t) campaign, including ^{200}Hg and ^{202}Hg, as a function of the number of valence nucleons N_{val}. The error bars include tentative assignments. In addition, the maximum number of sd IBM 0^+ states and the calculated number of 0^+ states below 3 MeV in this model using realistic parameters are plotted. Please refer to Ref. [9] for more details on the IBM calculations.
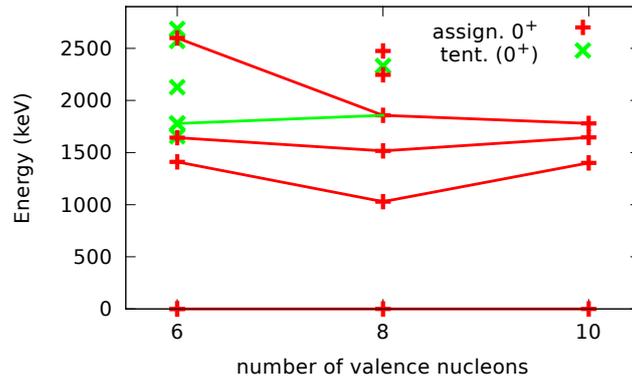
FIG. 6: (Color online) Energies of the firmly assigned 0^+ states up to 3 MeV for the isotopes ^{202}Hg, ^{200}Hg, and ^{198}Hg [9] investigated in this Q3D (p,t) campaign as a function of the number of valence nucleons N_{val}. Besides the larger number of low-lying 0^+ states and considering a (0^+) assignment in ^{202}Hg, the evolution of the 0^+_3 and 0^+_4 energies is pretty smooth. The comparison with the neighboring even Hg isotopes reveals a significant lowering of the 0^+_2 energy in ^{200}Hg at $N_{\mathrm{val}} = 8$.
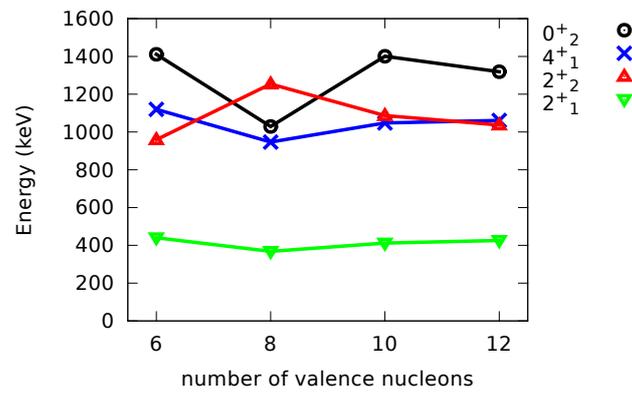
FIG. 7: (Color online) Systematic plot of low-energy states from ^{196}Hg to ^{202}Hg. One clearly notices the difference in the ^{200}Hg level scheme compared to the neighboring even Hg isotopes. The 0_2^+ energy is significantly lower and the 2_2^+ and 4_1^+ state diverge in ^{200}Hg. Figure adopted from Ref. [26].
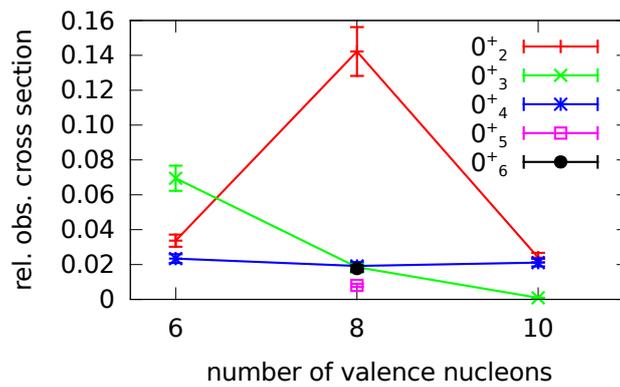
FIG. 8: (Color online) Relative observed cross section for 0_n^+ state assignments relative to the ground-state cross section $(\Sigma_i \sigma_n(i)/\Sigma_i \sigma_1(i)$, with $i = 5°, 17.5°$, or $30°$ and $n > 1$) as a function of the number of valence nucleons N_{val}. One notes the sharp rise of the relative cross section of the 0_2^+ state in ^{200}Hg at $N_{\text{val}} = 8$, whereas the other observed relative cross sections are significantly smaller and show a rather constant or smooth behavior with changing N_{val}.

Tables

TABLE I: $R(5/17.5)$ ratios and cross sections of firmly assigned 0^+ and tentatively assigned (0^+) states in ^{200}Hg. All states are discussed in detail in the text. New 0^+ state assignments are marked with an asterix, tentative (0^+) state assignments are denoted in *italic*.

Energy (keV)	$R(5/17.5)$	$\sigma(5°)$ (mb/sr)	$\sigma(17.5°)$ (mb/sr)
0.0 (0)	13.44 (37)	0.9819 (987)	0.0731 (75)
1029.3 (1)	4.78 (23)	0.1221 (125)	0.0256 (28)
1515.5 (3)	10.51 (123)	0.0202 (22)	0.0019 (3)
1856.6 (2)	7.95 (210)	0.0218 (24)	0.0027 (8)
2246.1 (2) *	4.97 (68)	0.0082 (10)	0.0016 (3)
2331.8 (3)	*3.19 (87)*	*0.0020 (4)*	*0.0006 (2)*
2475.2 (1) *	4.36 (46)	0.0163 (19)	0.0037 (5)

TABLE II: Summary of the observed peaks in the ^{200}Hg measurement and their cross sections. The measured cross sections have a 10% systematic uncertainty due to the beam-current normalization. The uncertainties on the relative $R(5/17.5)$ ratios are often smaller. Cross sections that were not observed because they were below the energy-dependent sensitivity limit of that particular run, which was around a few 10^{-4} mb, are listed as 0 mb/sr. Each listed state was carefully checked for the relevant $R(5/17.5)$ ratio by testing reasonable upper and lower limits for peaks with low statistics.

	Cross section (mb/sr)		
Energy (keV)	$\sigma(5°)$	$\sigma(17.5°)$	$\sigma(30°)$
-56.5 (11) [†]	0	0.0007 (3)	0
0.0 (0) [∗]	0.9819 (987)	0.0731 (75)	0.4843 (486)
367.9 (0) [∗]	0.0713 (74)	0.2079 (210)	0.1035 (105)
483.1 (2) [†]	0.0044 (7)	0.0007 (3)	0.0019 (3)
678.2 (4) [†]	0.0023 (5)	0.0006 (2)	0.0016 (3)
706.9 (3) [†]	0.0056 (8)	0.0005 (2)	0.0030 (4)
815.8 (7) [†]	0.0005 (2)	0.0002 (2)	0.0004 (2)
947.7 (1) [∗]	0.0123 (15)	0.0079 (10)	0.0043 (6)
1029.3 (1) [∗]	0.1221 (125)	0.0256 (28)	0.0711 (73)
1118.3 (8) [†]	0	0.0007 (3)	0
1158.3 (7) [†]	0.0006 (2)	0.0001 (1)	0.0003 (2)
1253.9 (1) [∗]	0.0137 (16)	0.0485 (51)	0.0261 (28)
1283.0 (7) [†]	0	0	0.0006 (2)
1353.4 (7)	0.0005 (2)	0.0001 (1)	0.0001 (1)
1503.5 (5)	0	0.0012 (2)	0.0008 (2)
1515.5 (3) [∗]	0.0202 (22)	0.0019 (3)	0.0062 (8)
1573.9 (1)	0.0483 (50)	0.1424 (143)	0.0695 (71)
1593.3 (5)	0.0012 (3)	0.0011 (2)	0
1619.7 (10)	0.0004 (2)	0.0001 (1)	0
1641.5 (4)	0.0022 (4)	0.0014 (2)	0.0010 (2)
1658.9 (0) [∗]	0.0972 (99)	0.0863 (87)	0.0995 (101)
1706.3 (1)	0.0019 (4)	0.0060 (7)	0.0082 (10)
1730.8 (3)	0.0069 (9)	0.0035 (4)	0.0017 (3)
1775.5 (5)	0.0005 (2)	0.0011 (2)	0
1794.6 (4) [†]	0	0.0009 (2)	0.0005 (2)
1851.0 (1)	0.0166 (19)	0.0352 (37)	0.0364 (39)
1856.6 (2)	0.0218 (24)	0.0027 (8)	0.0050 (10)
1882.9 (2) [∗]	0.0018 (5)	0.0068 (8)	0.0026 (4)
1919.4 (12)	0	0.0002 (1)	0
1961.9 (2)	0.0010 (3)	0.0014 (2)	0.0016 (3)
1971.6 (3)	0.0012 (3)	0.0017 (3)	0.0012 (3)
1978.4 (1)	0.0162 (18)	0.0165 (17)	0.0194 (21)
2000.9 (6)	0	0.0007 (2)	0.0005 (2)
2048.0 (7)	0	0	0.0007 (2)
2060.9 (3)	0.0011 (3)	0.0011 (2)	0.0007 (2)
2074.6 (2) [∗]	0.0098 (12)	0.0085 (9)	0.0103 (12)
2099.0 (1)	0.0099 (12)	0.0147 (16)	0.0194 (21)
2116.7 (2)	0.0011 (3)	0.0019 (3)	0.0009 (2)
2127.3 (3)	0.0010 (3)	0.0013 (2)	0.0008 (2)
2143.3 (1)	0.0026 (5)	0.0047 (6)	0.0072 (9)
2151.0 (1)	0.0091 (11)	0.0094 (10)	0.0068 (9)
2180.1 (3)	0	0.0010 (2)	0.0011 (3)
2190.8 (9)	0.0016 (3)	0.0020 (3)	0.0006 (2)
2222.7 (2)	0.0011 (3)	0.0015 (2)	0.0030 (5)
2228.6 (5)	0.0008 (3)	0.0006 (2)	0
2246.1 (2)	0.0082 (10)	0.0016 (3)	0.0024 (4)
2258.1 (5)	0	0	0.0010 (2)
2274.2 (1) [∗]	0.0077 (10)	0.0048 (6)	0.0045 (6)
2289.1 (1)	0.0108 (13)	0.0180 (19)	0.0101 (12)
2298.6 (1)	0.0036 (6)	0.0045 (6)	0.0066 (8)
2307.8 (2)	0.0009 (3)	0.0026 (4)	0.0038 (5)
2321.6 (2)	0.0030 (5)	0.0034 (4)	0.0038 (5)
2331.8 (3)	0.0020 (4)	0.0006 (2)	0
2343.7 (2)	0.0038 (6)	0.0107 (12)	0.0048 (6)
2377.2 (1)	0.0112 (13)	0.0134 (14)	0.0187 (20)
2388.7 (1) [∗]	0.0218 (24)	0.0633 (64)	0.0274 (29)
2414.1 (9)	0.0020 (4)	0.0047 (6)	0.0096 (11)
2463.7 (4)	0.0005 (2)	0.0008 (2)	0.0009 (3)
2475.2 (1)	0.0163 (19)	0.0037 (5)	0.0072 (9)
2480.3 (1)	0.0051 (9)	0.0055 (7)	0.0076 (10)
2485.7 (2)	0.0017 (4)	0.0036 (5)	0.0040 (7)

2490.9 (4)	0.0014 (3)	0.0007 (2)	0.0003 (3)
2514.0 (4)	0	0.0003 (1)	0.0008 (3)
2524.6 (7)	0	0	0.0007 (2)
2548.1 (2)	0.0034 (5)	0.0024 (4)	0.0022 (4)
2565.6 (1)	0.0074 (9)	0.0078 (9)	0.0094 (12)
2610.4 (1)	0.0070 (9)	0.0076 (9)	0.0060 (8)
2621.1 (6)	0	0	0.0009 (3)
2643.7 (2)	0.0021 (4)	0.0009 (2)	0.0014 (3)
2661.9 (1)	0.0109 (13)	0.0119 (13)	0.0158 (18)
2679.8 (2)	0.0011 (3)	0.0027 (4)	0.0030 (5)
2691.7 (4)	0.0036 (6)	0.0094 (11)	0
2697.5 (1)	0.0070 (9)	0.0092 (11)	0.0088 (11)
2715.4 (5)	0	0.0009 (2)	0.0010 (3)
2729.9 (4)	0.0034 (5)	0.0063 (8)	0.0113 (13)
2736.8 (2)	0.0042 (6)	0.0132 (15)	0.0061 (9)
2762.8 (3) [*]	0.0016 (3)	0.0018 (3)	0.0020 (3)
2773.5 (4)	0.0033 (5)	0.0030 (4)	0.0022 (4)
2786.7 (23)	0.0011 (3)	0.0007 (4)	0.0011 (3)
2793.5 (8)	0.0026 (4)	0.0022 (4)	0.0009 (2)
2828.2 (3)	0.0012 (3)	0.0014 (2)	0.0015 (3)
2841.9 (2)	0.0019 (4)	0.0030 (4)	0.0028 (4)
2862.9 (2)	0.0068 (9)	0.0089 (10)	0.0068 (9)
2880.6 (2)	0.0137 (16)	0.0115 (13)	0.0091 (11)
2907.6 (21)	0	0.0015 (3)	0.0007 (2)

----

[*] This state was used for energy calibration using the published ^{200}Hg excitation energy from the data sheets [16].
[†] Identified contaminant from target impurity.
[‡] Very likely an unidentified contaminant.

TABLE III: $R(5/17.5)$ ratios and cross sections of firmly assigned 0^+ and tentatively assigned (0^+) states in ^{202}Hg. All states are discussed in detail in the text. New 0^+ state assignments are marked with an asterix, tentative (0^+) state assignments are denoted in *italic*.

Energy (keV)	$R(5/17.5)$	$\sigma(5°)$ (mb/sr)	$\sigma(17.5°)$ (mb/sr)
0.1 (1)	15.67 (42)	0.8949 (897)	0.0571 (59)
1411.0 (3)	12.26 (181)	0.0280 (30)	0.0023 (4)
1643.0 (3)	7.34 (45)	0.0615 (63)	0.0084 (10)
1655.8 (13)	*3.08 (126)*	*0.0019 (5)*	*0.0006 (2)*
1778.9 (6)	*4.53 (154)*	*0.0021 (4)*	*0.0005 (2)*
2126.7 (7)	*3.17 (168)*	*0.0015 (3)*	*0.0005 (2)*
2570.7 (10)	*2.32 (247)*	*0.0006 (2)*	*0.0002 (2)*
2598.5 (2) *	4.25 (39)	0.0200 (22)	0.0047 (6)
2685.7 (5)	*4.70 (322)*	*0.0017 (3)*	*0.0004 (2)*

TABLE IV: Summary of the observed peaks in the ^{202}Hg measurement and their cross sections. The determined cross sections have a 10% systematic uncertainty due to the beam-current normalization. The uncertainties on the relative $R(5/17.5)$ ratios are often smaller. Cross sections that were not observed because they were below the energy-dependent sensitivity limit of that particular run, which was around a few 10^{-4} mb, are listed as 0 mb/sr. Each listed state was carefully checked for the relevant $R(5/17.5)$ ratio by testing reasonable upper and lower limits for peaks with low statistics.

		Cross section (mb/sr)	
Energy (keV)	$\sigma(5°)$	$\sigma(17.5°)$	$\sigma(30°)$
0.1 (1) [∗]	0.8949 (897)	0.0571 (59)	0.4043 (405)
439.4 (1) [∗]	0.1116 (114)	0.3439 (346)	0.1558 (157)
496.3 (4) [†]	0.0538 (56)	0.0036 (5)	0.0238 (25)
864.6 (1) [†]	0.0035 (5)	0.0107 (13)	0.0051 (6)
960.2 (1) [∗]	0.0173 (19)	0.0380 (40)	0.0216 (23)
979.8 (4) [†]	0.0027 (5)	0.0007 (2)	0.0009 (2)
1120.0 (1)	0.0151 (17)	0.0188 (21)	0.0189 (20)
1174.6 (6) [†]	0.0017 (3)	0	0.0011 (2)
1182.5 (4)	0	0.0015 (3)	0.0011 (2)
1202.6 (2) [†]	0.0079 (10)	0.0004 (2)	0.0044 (5)
1311.5 (0) [∗]	0.2361 (238)	0.1793 (181)	0.1298 (131)
1347.5 (3)	0.0012 (3)	0.0011 (3)	0.0007 (2)
1389.3 (2)	0.0018 (3)	0.0065 (8)	0.0010 (2)
1411.0 (3) [∗]	0.0280 (30)	0.0023 (4)	0.0154 (16)
1443.5 (5) [†]	0.0008 (2)	0	0.0003 (1)
1525.5 (2) [†]	0.0069 (8)	0.0014 (3)	0.0042 (5)
1564.6 (2)	0.0113 (13)	0.0102 (12)	0.0120 (13)
1575.7 (1) [∗]	0.0096 (11)	0.0253 (27)	0.0114 (12)
1624.0 (1)	0.0031 (5)	0.0043 (5)	0.0076 (9)
1643.0 (3) [∗]	0.0615 (63)	0.0084 (10)	0.0244 (25)
1655.8 (13)	0.0019 (5)	0.0006 (2)	0.0014 (3)
1678.3 (2) [∗]	0.0012 (3)	0.0032 (4)	0.0023 (3)
1724.0 (6)	0	0.0004 (1)	0.0007 (2)
1748.2 (9)	0.0023 (4)	0.0029 (4)	0.0017 (3)
1778.9 (6)	0.0021 (4)	0.0005 (2)	0.0013 (2)
1794.1 (1) [∗]	0.0457 (47)	0.1645 (166)	0.0821 (83)
1823.2 (1) [∗]	0.0166 (18)	0.0256 (27)	0.0109 (12)
1861.5 (3)	0	0.0027 (4)	0.0007 (2)
1903.1 (4)	0.0025 (4)	0.0016 (3)	0.0022 (3)
1965.4 (1)	0.0220 (24)	0.0380 (39)	0.0463 (47)
1988.4 (1)	0.0011 (2)	0.0033 (5)	0.0058 (7)
2011.5 (4) [†]	0.0014 (3)	0	0.0005 (1)
2060.1 (2)	0.0013 (3)	0.0021 (4)	0.0028 (4)
2071.4 (1) [∗]	0.0476 (49)	0.1206 (122)	0.0629 (64)
2111.8 (1)	0.0063 (8)	0.0271 (28)	0.0378 (39)
2126.7 (7)	0.0015 (3)	0.0005 (2)	0.0017 (3)
2134.1 (1)	0.0137 (15)	0.0103 (11)	0.0098 (11)
2155.6 (2)	0.0054 (7)	0.0045 (6)	0.0054 (6)
2196.3 (4)	0.0013 (3)	0.0007 (2)	0
2205.5 (3)	0.0125 (14)	0.0056 (7)	0.0015 (3)
2223.5 (1)	0.0053 (7)	0.0085 (10)	0.0132 (14)
2250.5 (4)	0	0.0005 (2)	0.0014 (2)
2280.5 (2)	0.0049 (6)	0.0131 (14)	0.0052 (6)
2294.7 (2)	0.0049 (6)	0.0113 (13)	0.0056 (7)
2309.9 (3) [∗]	0.0015 (3)	0.0008 (2)	0.0014 (3)
2322.9 (6)	0	0.0005 (2)	0.0004 (1)
2342.1 (2)	0.0047 (6)	0.0044 (6)	0.0041 (5)
2357.9 (2)	0.0120 (14)	0.0128 (14)	0.0112 (12)
2371.9 (2)	0.0019 (3)	0.0053 (7)	0.0029 (4)
2415.4 (8)	0	0.0005 (2)	0
2427.5 (8)	0	0.0005 (2)	0.0004 (2)
2441.1 (2)	0.0072 (9)	0.0094 (11)	0.0134 (15)
2461.7 (2)	0.0037 (5)	0.0055 (7)	0.0071 (8)
2473.4 (4)	0.0013 (3)	0.0013 (3)	0.0013 (3)
2515.6 (2) [∗]	0.0075 (9)	0.0057 (7)	0.0031 (5)
2550.3 (2)	0.0108 (12)	0.0142 (15)	0.0095 (12)
2560.1 (2)	0.0079 (10)	0.0096 (11)	0.0119 (14)
2570.7 (10)	0.0006 (2)	0.0002 (2)	0
2584.6 (5)	0.0012 (2)	0.0009 (2)	0.0015 (3)
2598.5 (2)	0.0200 (22)	0.0047 (6)	0.0070 (8)
2605.0 (4)	0.0029 (5)	0.0037 (5)	0.0059 (7)

2639.1 (15)	0.0005 (2)	0	0.0007 (2)
2652.9 (3)	0.0058 (7)	0.0103 (12)	0.0042 (6)
2675.7 (3)	0.0067 (8)	0.0096 (11)	0.0106 (13)
2685.7 (5)	0.0017 (3)	0.0004 (2)	0
2708.5 (3)	0.0063 (8)	0.0073 (9)	0.0044 (7)
2731.4 (3) [*]	0.0074 (9)	0.0146 (17)	0.0161 (17)
2748.2 (3)	0.0033 (6)	0.0162 (19)	0.0068 (8)
2755.0 (3)	0.0218 (24)	0.0265 (29)	0.0323 (34)
2781.7 (3)	0.0019 (3)	0.0030 (5)	0.0032 (5)
2814.7 (6)	0	0.0016 (3)	0.0015 (3)
2824.8 (3)	0.0089 (10)	0.0156 (17)	0.0123 (15)
2847.8 (4)	0.0017 (3)	0.0025 (4)	0.0025 (5)
2872.2 (4)	0.0009 (2)	0.0012 (3)	0.0016 (4)
2882.4 (5)	0.0017 (3)	0.0052 (7)	0.0032 (5)
2906.2 (18)	0.0026 (4)	0.0059 (8)	0.0029 (5)
2923.8 (4)	0.0179 (19)	0.0186 (21)	0.0191 (22)
2934.0 (8)	0.0070 (8)	0.0077 (10)	0.0065 (10)

[*] This state was used for energy calibration using the published ^{202}Hg excitation energy from the data sheets [17].
[†] Identified contaminant from target impurity.